

# The Structural Effects of Rotation in Low Mass Stars

Alison Sills, M. H. Pinsonneault

Department of Astronomy, The Ohio State University, 174 W. 18th Ave., Columbus, OH,  
43210, USA

## ABSTRACT

We present theoretical models of rotating low mass stars ( $0.1 - 1.0 M_{\odot}$ ) to demonstrate the effect of rotation on the effective temperature and luminosity of stars. The range of rotation rates in our models corresponds to the observed rotation rates in young low mass stars. Rotation lowers the effective temperature and luminosity of the models relative to standard models of the same mass and composition. We find that the decrease in  $T_{eff}$  and  $L$  can be significant at the higher end of our mass range, but becomes small below  $0.4 M_{\odot}$ . The effects of different assumptions about internal angular momentum transport are discussed. Formulae for relating  $T_{eff}$  to mass and  $v_{rot}$  are presented. We demonstrate that the kinetic energy of rotation is not a significant contribution to the luminosity of low mass stars.

*Subject headings:* stars: evolution – stars: rotation – stars: interiors – stars: formation – low mass stars

## 1. Introduction

We are now able to observe stars with regularity down to the hydrogen burning limit in open clusters (e.g. NGC 2420, von Hippel *et al.* 1996), globular clusters (e.g. 47 Tucanae, Santiago, Elson & Gilmore 1996), and the field (e.g. Tinney, Mould & Reid 1993). We have also been able to observe rotation in these stars, using spectroscopy (Kraft 1965, Stauffer *et al.* 1997) to determine  $v \sin i$ , and also using photometry to monitor spot modulation on the stars (Barnes & Sofia 1999, Prosser *et al.* 1995) and thereby determine rotational periods. This plethora of information about the rotation of low mass stars has been a great boon to the study of these stars for a number of reasons. First of all, the rotation rates of stars on the main sequence are determined by their pre-main sequence evolution, so that by studying the rotational evolution of low mass stars, we can investigate the early stages of stellar evolution. Secondly, stellar rotation is tied to stellar magnetic phenomena. The

evolution of the rotation rates is largely determined by angular momentum loss from a magnetized stellar wind (Kawaler 1988, Weber & Davis 1967). Stellar rotation is found to correlate with chromospheric activity and other magnetic tracers (for a review see Hartmann & Noyes 1987), which lends support to the idea that rotation plays a crucial role in the generation of stellar magnetic fields, perhaps through a dynamo.

The major obstacles which prevented us from modeling very low mass stars accurately in the past have been the lack of adequate model atmospheres, opacities and equations of state for low temperatures (less than 4000 K). Lately, however, several groups (Alexander & Ferguson 1994; Allard & Hauschildt 1995; Saumon, Chabrier & Van Horn 1995) have made breakthroughs in the necessary physics. Improved evolutionary models of very low mass stars have been produced over the last few years (Baraffe *et al.* 1998). However, the effects of rotation have not been included in these recent low mass models, and neglecting it could lead to anomalous results. For example, rotation can modify the amount of lithium depletion in low mass stars, affecting the derived ages from lithium isochrone fitting (e.g. Stauffer, Schultz & Kirkpatrick 1998). In this work, we present the first rotational models of stars less massive than  $0.5 M_{\odot}$  and examine the structural effects of rotation in these stars. In section 2, we present the method used to determine the rotational evolution of the low mass stars. We present the results in section 3, and discuss their implications in section 4.

## 2. Method

We used the Yale Rotating Stellar Evolution Code (YREC) to construct models of the low mass stars. YREC is a Henyey code which solves the equations of stellar structure in one dimension (Guenther *et al.* 1992). The star is treated as a set of nested, rotationally deformed shells. Nuclear reaction rates are taken from Gruzinov & Bahcall (1998). The initial chemical mixture is the solar mixture of Grevesse & Noels (1993), and our models have a metallicity of  $Z=0.0188$ . We use the latest OPAL opacities (Iglesias & Rogers 1996) for the interior of the star down to temperatures of  $\log T(K) = 4$ . For lower temperatures, we use the molecular opacities of Alexander & Ferguson (1994). For regions of the star which are hotter than  $\log T(K) \geq 6$ , we used the OPAL equation of state (Rogers, Swenson & Iglesias 1996). For regions where  $\log T(K) \leq 5.5$ , we used the equation of state from Saumon, Chabrier & Van Horn (1995), which calculates particle densities for hydrogen and helium including partial dissociation and ionization by both pressure and temperature. In the transition region between these two temperatures, both formulations are weighted with a ramp function and averaged. The equation of state includes both radiation pressure

and electron degeneracy pressure. For the surface boundary condition, we used the stellar atmosphere models of Allard & Hauschildt (1995), which include molecular and grain effects and are therefore relevant for low mass stars. We used the standard Böhm-Vitense convective mixing length theory (Cox 1968; Böhm-Vitense 1958) with  $\alpha=1.72$ . This value of  $\alpha$ , as well as the solar helium abundance,  $Y_{\odot} = 0.273$ , was obtained by calibrating models against the observed radius ( $6.9598 \times 10^{10}$  cm) and luminosity ( $3.8515 \times 10^{33}$  erg/s) at the present age of the Sun (4.57 Gyr).

The structural effects of rotation are treated using the scheme derived by Kippenhahn & Thomas (1970) and modified by Endal & Sofia (1976). The details of this particular implementation are discussed in Pinsonneault *et al.* (1989). In summary, quantities are evaluated on equipotential surfaces rather than the spherical surfaces usually used in stellar models. The mass continuity equation is not altered by rotation:

$$\frac{\partial M}{\partial r} = 4\pi r^2 \rho. \quad (1)$$

The equation of hydrostatic equilibrium includes a term which takes into account the modified gravitational potential of the non-spherical equipotential surface:

$$\frac{\partial P}{\partial M} = -\frac{GM}{4\pi r^4} f_P, \quad (2)$$

where

$$f_P = \frac{4\pi r^4}{GM S} \frac{1}{\langle g^{-1} \rangle}, \quad (3)$$

and

$$\langle g^{-1} \rangle = \frac{1}{S} \int_{\psi=const} g^{-1} d\sigma, \quad (4)$$

$S$  is the surface area of an equipotential surface, and  $d\sigma$  is an element of that surface. The factor  $f_P$  is less than one for non-zero rotation, and approaches one as the rotation rate goes to zero. The radiative temperature gradient also depends on rotation:

$$\frac{\partial \ln T}{\partial \ln P} = \frac{3\kappa}{16\pi acG} \frac{P}{T^4} \frac{L}{M} \frac{f_T}{f_P}, \quad (5)$$

where

$$f_T = \left( \frac{4\pi r^2}{S} \right)^2 \frac{1}{\langle g \rangle \langle g^{-1} \rangle} \quad (6)$$

and  $\langle g \rangle$  is analogous to  $\langle g^{-1} \rangle$ .  $f_T$  has the same asymptotic behaviour as  $f_P$ , but is typically much closer to 1.0. The energy conservation equation retains its non-rotating form.

Therefore, all the structural effects of rotation are limited to the equation of hydrostatic

equilibrium and the radiative temperature gradient. This modified temperature gradient is used in the Schwarzschild criterion for convection:

$$\frac{\partial \ln T}{\partial \ln P} = \min \left[ \nabla_{ad}, \nabla_{rad} \frac{f_T}{f_P} \right] \quad (7)$$

where  $\nabla_{ad}$  and  $\nabla_{rad}$  are the normal spherical adiabatic and radiative temperature gradients

We start our models on the birthline of Palla & Stahler (1991), which is the deuterium-burning main sequence and corresponds to the upper envelope of T Tauri observations in the HR diagram. It has been shown (Barnes & Sofia 1996) that this physically realistic assumption for the initial conditions of stellar rotation models is crucial for accurate modeling of ultra-fast rotators in young clusters. All our models started with an initial period of 8 days, which corresponds to the median classical T Tauri star rotation period (Choi & Herbst 1996).

In this paper, we present stellar models for solar metallicity stars between 0.1 and 1.0  $M_{\odot}$  in increments of 0.1  $M_{\odot}$ . These models have been evolved from the birthline to an age of 10 Gyr. We have not considered any angular momentum loss, since in this paper we wish to explore the largest reasonable structural changes caused by rotation. In our standard models, local conservation of angular momentum is enforced in radiative regions of the star, and convective zones rotate as solid bodies. We have also calculated models in which solid body rotation is enforced throughout the star, regardless of the convective state of the region.

### 3. Results

The initial rotation period of 8 days for our models was chosen because those models represent the maximum observed rotation rates for stars in young open clusters. Observed rotation rates as a function of effective temperature are plotted in figure 1, along with our rotating models at the zero-age main sequence. The data shown here are from five young clusters: IC 2602 and IC 2391 (30 Myr),  $\alpha$  Persei (50 Myr), Pleiades (70 Myr) and Hyades (600 Myr), and were obtained from the Open Cluster Database (Prosser & Stauffer). To transform between the observed V-I colours and  $T_{eff}$ , we used the empirical colour calibration of Yuan *et al.* (1999). Our models are rotating at or slightly above the fastest rotation rates observed in these representative clusters.

The evolutionary tracks for both rotating and non-rotating models are presented in figure 2. As expected (Sackmann 1970, Pinsonneault *et al.* 1989), the effect of rotation is to shift stars to lower effective temperatures and lower luminosities, mimicking a star of

lower mass. This effect is most pronounced for the highest mass stars presented in this paper, and is reduced to a low level for stars less than  $0.4 M_{\odot}$ . Since low mass stars are fully convective, their temperature gradient will be the adiabatic gradient, which does not depend on rotation rate (equation 7). However, the structural effects of rotation are still apparently in fully convective stars, and diminish with decreasing mass. This suggests that an additional mechanism is also at work. As stars get less massive, their central pressure is being provided less by thermal pressure and more by degeneracy pressure. The amount of degeneracy is determined by the density in the interior, which is not affected by rotation (see equation 1). Rotation provides an additional method of support for the star, but in stars with a significant amount of degeneracy, the rotational support is a smaller fraction of the total pressure. Therefore, the structure of the low mass stars is less affected by rotation than their higher mass counterparts.

Figure 3 compares the evolutionary tracks for rotating stars under different assumptions about internal angular momentum transport. The solid tracks are stars which have differentially rotating radiative cores and rigidly rotating convection zones, while the dashed lines show the tracks for stars which are constrained to rotate as solid bodies. The two tracks for each mass have the same surface rotation rate at the zero-age main sequence. The low mass stars show no difference between the two assumptions, since these stars are fully convective for the entire 10 Gyr plotted here. Therefore, they always rotate as solid bodies. The higher mass stars begin their lives high on the pre-main sequence as fully convective, solid body rotators. As they contract and develop radiative cores, however, the difference in the two assumptions about angular momentum transport becomes apparent. Differential rotators have a higher total angular momentum than solid body rotators of the same surface rotation rate. As stars contract along the pre-main sequence, they become more centrally concentrated, which means that the core spins up more than the envelope does. The solid body rotators are forced to spread their angular momentum evenly throughout the star, so they have less total angular momentum for a given surface rotation rate. Therefore, the impact of rotation on the structure of the star is larger for differential rotators than for solid body rotators of the same surface rotation rate. However, at constant initial angular momentum, the solid body rotators are cooler at the zero age main sequence, and have longer pre-main sequence lifetimes, than differentially rotating stars of the same mass. When comparing the effects of rotation between different models, it is important to note whether the comparison is between stars with the same current surface rotation rate, or with the same initial angular momentum.

We included the kinetic energy of rotation ( $T = \frac{1}{2}I\omega^2$ ) in our determination of the total luminosity in each shell of the star. As the star changes its moment of inertia  $I$  and its rotation rate  $\omega$ , the resulting change in its rotational kinetic energy can be included in the

energy budget of the star. Most implementations of stellar rotation into stellar structure and evolution neglect this energy since it is expected that the amount of kinetic energy available is not enough to significantly affect the evolution of the star. Since very low mass stars have much lower luminosities than solar-mass stars, but their moments of inertia are not as significantly lower, it is plausible that the kinetic energy of rotation would contribute a significant fraction of the total luminosity of the star. As shown in figure 4, however, the change in the kinetic energy of rotation contributes no more than 6% of the total luminosity of the star in the  $1.0 M_{\odot}$  model, and that contribution lasts less than 50 Myr. As expected, the lowest mass star has the most significant contribution, lasting for about 1 Gyr, but at 4% or less. The positions of stars in the HR diagram are minimally affected by the inclusion of this source of energy. The kinetic energy of rotation reduces the luminosity at any given time by less than 0.02 dex in  $\log(L/L_{\odot})$ , and usually less than 0.005 dex. The timescales for evolution are also equally unaffected. The models presented in this paper, those with no angular momentum loss, will have the maximum possible effect of rotational kinetic energy. Since these models show no significant effect, we conclude that the change in the kinetic energy of rotation is at most a perturbation on the structure.

The main structural effect of rotation is a reduction in the effective temperature of stars. Using our tracks, we have quantified the relationship between rotational velocity and the difference in effective temperature at the zero age main sequence. In figure 5 we present this relationship for stars of different masses, and for both the differentially rotating (solid lines) and solid body models (dashed lines). For low mass stars, the difference in temperature caused by rotation is of order a few tens of degrees (and reduces to less than 10 degrees for stars of  $0.2 M_{\odot}$ ). This difference is therefore negligible. However, the reduction in effective temperature is larger for the more massive stars, and can reach significant levels of a few hundred degrees for stars more massive than about  $0.6 M_{\odot}$ . Therefore, when determining masses from observed temperatures or colours, it is important know how fast these stars are rotating. The relationship between rotation rate and difference in effective temperature, for a given stellar mass, is well-fit by a polynomial. The coefficients for this polynomial at different masses and under different assumptions of internal angular momentum transport are given in table 2. It should be noted that while solid body rotators of the same initial period rotate faster at the zero age main sequence than differentially rotating stars, the structural effects of rotation are slightly more pronounced in the differential rotators at constant rotation speed. Therefore, for a constant rotational velocity, stars which rotate differentially have a higher angular momentum than solid body rotators.

For stars of the same mass, rotation reduces the luminosity of stars as well as their temperatures. The different in luminosity is not as important as the difference in temperature cause by rapid rotation, as shown in figure 6. Even for the most extreme case,

the difference in luminosity for a  $1.0 M_{\odot}$  star rotating at 250 km/s is less than 0.12 dex in  $\log(L_{\odot})$ . While differences of this size will result in a thicker main sequence of a cluster, it should not affect any scientific results significantly. Most stars in clusters do not rotate very fast, so the upper main sequence will be well-defined for any isochrone fitting or distance determination. Luminosity is used as an indicator of mass for low mass stars, but since the difference in luminosity between rapid rotators and non-rotators is very small for low mass stars, this calibration should not be affected by rotation.

The total effect of rotation is such that the locus of the zero age main sequence becomes brighter as stars rotate more quickly. The combination of a significant decrease in temperature with a small decrease in luminosity for stars of the same mass moves the locus above the non-rotating main sequence. At a surface rotation rate of 100 km/s, the rotating main sequence is brighter by about 0.01 magnitudes. At 200 km/s, the sequence is brighter by 0.03 magnitudes. Therefore, we expect to see rapid rotators in clusters lying above the cluster main sequences by a few hundredths of a magnitude.

Since they are fainter, rapid rotators have slightly longer lifetimes compared to non-rotating stars of the same mass. The amount of increase depends on the mass of the star and the rotation rate, but in the most extreme case ( $1.0 M_{\odot}$  rotating at 250 km/s), the difference in pre-main sequence lifetime is 7%. For rotation rates less than 100 km/s, the increase in lifetime is less than 1% for all masses.

#### 4. Summary and Discussion

We have investigated the effect of rotation on the structure of low mass stars. We discussed a number of implications, based on models which demonstrate the maximum extent of the differences between rotating and non-rotating models. The most important effect is the reduction of effective temperature for stars of a given mass. Rapid rotators are cooler than slow rotators, and so, for stars more massive than  $0.5 M_{\odot}$ , any relationship between temperature and mass should take into account the rotation rate of the star. We have shown that the structural effects of rotation in very low mass stars (less than  $\sim 0.5 M_{\odot}$ ) are minimal and can be neglected when interpreting temperatures and luminosities of these stars from observations. Table 2 gives the polynomial correction between the effective temperature of a rotating star and that of a non-rotating star, as a function of rotation rate and stellar mass.

We have shown that the kinetic energy of rotation is not a significant contribution to the total luminosity of stars between  $0.1$  and  $1.0 M_{\odot}$ , and does not change the timescale

for evolution on the pre-main sequence. This rotational contribution to the total energy of the star can therefore be neglected in future evolutionary calculations.

Stellar activity can also influence the color-temperature relationship; because of the well-known correlation between increased rotation, increased stellar spot coverage, and increased chromospheric activity this will tend to change the observed position of rapidly rotating stars in the HR diagram relative to slow rotators. Different color indices are affected to different degrees; for example, Fekel, Moffett, & Henry (1986) found a systematic departure between the B-V and V-I colors of active stars. Stars with more modest activity levels have a more normal color-color relationship (e.g. Rucinski 1987). Active stars tend to be bluer in B-V than in V-I relative to less active stars. Fekel, Moffett, & Henry (1986) treated this as an infrared excess, but in open clusters such as the Pleiades and Alpha Per rapid rotators are on or above the main sequence in V-I, but can be below the zero-age main sequence in B-V (Pinsonneault et al. 1998). Given the theoretical trends presented here, this suggests that V-I is a good tracer of temperature, and that B-V is the colour which is most affected by activity. The difference between effective temperatures based on B-V and those based on V-I can reach 200 K in Pleiades stars (Krishnamurthi, Pinsonneault, King, and Sills 1999).

In this work, we have neglected angular momentum loss, since we wish to demonstrate the maximum effects of rotation on the structure of low mass stars. However, angular momentum loss is required to explain the evolution of rotation rates observed by comparing stars of the same masses in open clusters of different ages (Barnes & Sofia 1996, Krishnamurthi *et al.* 1997). We have also chosen only two form of internal angular momentum transport in these models. Our models either enforced the local conservation of angular momentum in radiative regions, and enforce solid body rotation in convection zones, or we assume the entire star rotates as a solid body. We have not investigated the case in which local conservation of angular momentum is enforced throughout the star, nor have we included any transport of angular momentum caused by any internal instabilities. More detailed models, which include both angular momentum loss and a more complicated treatment of internal angular momentum transport, are needed to accurately model the structure and evolution of rotating stars. However, these complicated models will follow the same trends described in this work, with effects of the same magnitude or less. This paper therefore provides a useful guide to the effects of rotation on the structure of low mass stars.

This work was supported by NASA grant NAG5-7150. A. S. wishes to recognize support from the Natural Sciences and Engineering Research Council of Canada. We would like to acknowledge use of the Open Cluster Database, as provided by C.F. Prosser (deceased) and J.R. Stauffer, and which currently may be accessed at <http://cfa->



www.harvard.edu/~stauffer/, or by anonymous ftp to cfa0.harvard.edu (131.142.10.30), cd /pub/stauffer/clusters/.

## REFERENCES

- Alexander, D. R., & Ferguson, J. W. 1994, ApJ, 437, 879
- Allard, F., & Hauschildt, P. H. 1995, ApJ, 445, 433
- Baraffe, I., Chabrier, G., Allard, F., & Hauschildt, P. H. 1998, A&A, 337, 403
- Barnes, S., & Sofia. S. 1996, ApJ, 462, 746
- Barnes, S., & Sofia. S. 1999, preprint
- Böhm-Vitense, E. 1958, Zs. f. Ap., 46, 108
- Choi, P. I., & Herbst, W. 1996, AJ, 111, 283
- Cox, J. P. 1968, Principles of Stellar Structure, in two volumes (New York: Gordon and Breach)
- Endal, A. S., & Sofia, S. 1976, ApJ, 210, 184
- Fekel, F. C., Moffett, T. J., & Henry, G. W. 1986, ApJS, 60, 551
- Grevesse, N., & Noels, 1993, A. in Origin and Evolution of the Elements, ed. N. Prantzos, E. Vangioni-Flam, & M. Cassé (Cambridge:Cambridge Univ. Press), 15
- Gruzinov, A., & Bahcall, J. 1998, ApJ, 504, 996
- Guenther, D. B., Demarque, P., Kim, Y.-C., & Pinsonneault, M. H. 1992, ApJ, 387, 372
- Hartmann, L. W., & Noyes, R. N. 1987, ARA&A, 25, 271
- Iglesias, C. A., & Rogers F. J., 1996 ApJ, 464, 943
- Kawaler, S. D. 1988, ApJ, 333, 236
- Kippenhahn, R., & Thomas, H.-C. 1970 in *Stellar Rotation*, ed. A. Slettebak (Dordrecht: Reidel), p. 20
- Kraft, R. 1965, ApJ, 370, L39
- Krishnamurthi, A., Pinsonneault, M. H., Barnes, S., Sofia, S. 1997, ApJ, 480, 303
- Krishnamurthi, A., Pinsonneault, M. H., King, J. R., & Sills, A., 1999, in preparation
- Martin, E. L. & Claret, A. 1996, A&A, 306, 408
- Mendes, L. T. S., D'Antona, F., & Mazzitelli, I. 1999, A&A, 341, 174
- Pinsonneault, M. H., Kawaler, S. D., Sofia, S., & Demarque, P. D. 1990, ApJ, 338, 424

- Pinsonneault, M. H., Stauffer, J., Soderblom, D. R., King, J. R., & Hanson, R. B. 1998  
ApJ, 504, 170
- Prosser, C. F., Shetrone, M. D., Dasgupta, A., Backman, D. E., Laaksonen, b. D., Baker,  
S. W., Marschall, L. A., Whitney, B. A., Kuijken, K., & Stauffer, J. R. 1995, PASP,  
107, 211
- Prosser, C. F., & Stauffer, J. *The Open Cluster Database*, [http://cfa-  
www.harvard.edu/~stauffer/opencl/index.html](http://cfa-www.harvard.edu/~stauffer/opencl/index.html)
- Rogers, F. J., Swenson, F. J., & Iglesias, C. A. 1996, ApJ, 456, 902
- Rucinski, S. M. 1987, PASP, 99, 288
- Sackman, I.J. 1970, A&A, 8, 76
- Santiago, B., Elson, R., & Gilmore, G. 1996, MNRAS, 281, 1363
- Saumon, D., Chabrier, G., & Van Horn, H. M. 1995, ApJS, 99, 713
- Stauffer, J. R., Balachandran, S. C., Krishnamurthi, A., Pinsonneault, M., Terndrup, D.  
M., Stern, R. A. 1997, ApJ, 475, 604
- Stauffer, J. R., Schultz, G., Kirkpatrick, J. D. 1998, ApJ, 499, L199
- Tinney, C. G., Mould, J. R., & Reid, I. N. 1993, AJ, 105, 1045
- von Hippel, T., Gilmore, G., Tanvir, N., Robinson, D., & Jones, D. H. P. 1996, AJ, 112, 192
- Weber, E. J., & Davis, L., Jr. 1967, ApJ, 148, 217
- Yuan, Y., Pinsonneault, M. H., & Terndrup, D. 1999, in preparation

Fig. 1.— Observed rotation rates as a function of temperature for five young open clusters: IC 2602 and IC 2391 (30 Myr),  $\alpha$  Persei (50 Myr), Pleiades (70 Myr) and Hyades (600 Myr). The data are from the Open Cluster Database (Prosser & Stauffer). The solid line shows differentially rotating models with initial rotation periods of 8 days and masses between  $1.0$  and  $0.1 M_{\odot}$ . These models represent the fastest observed rotators in young open clusters.

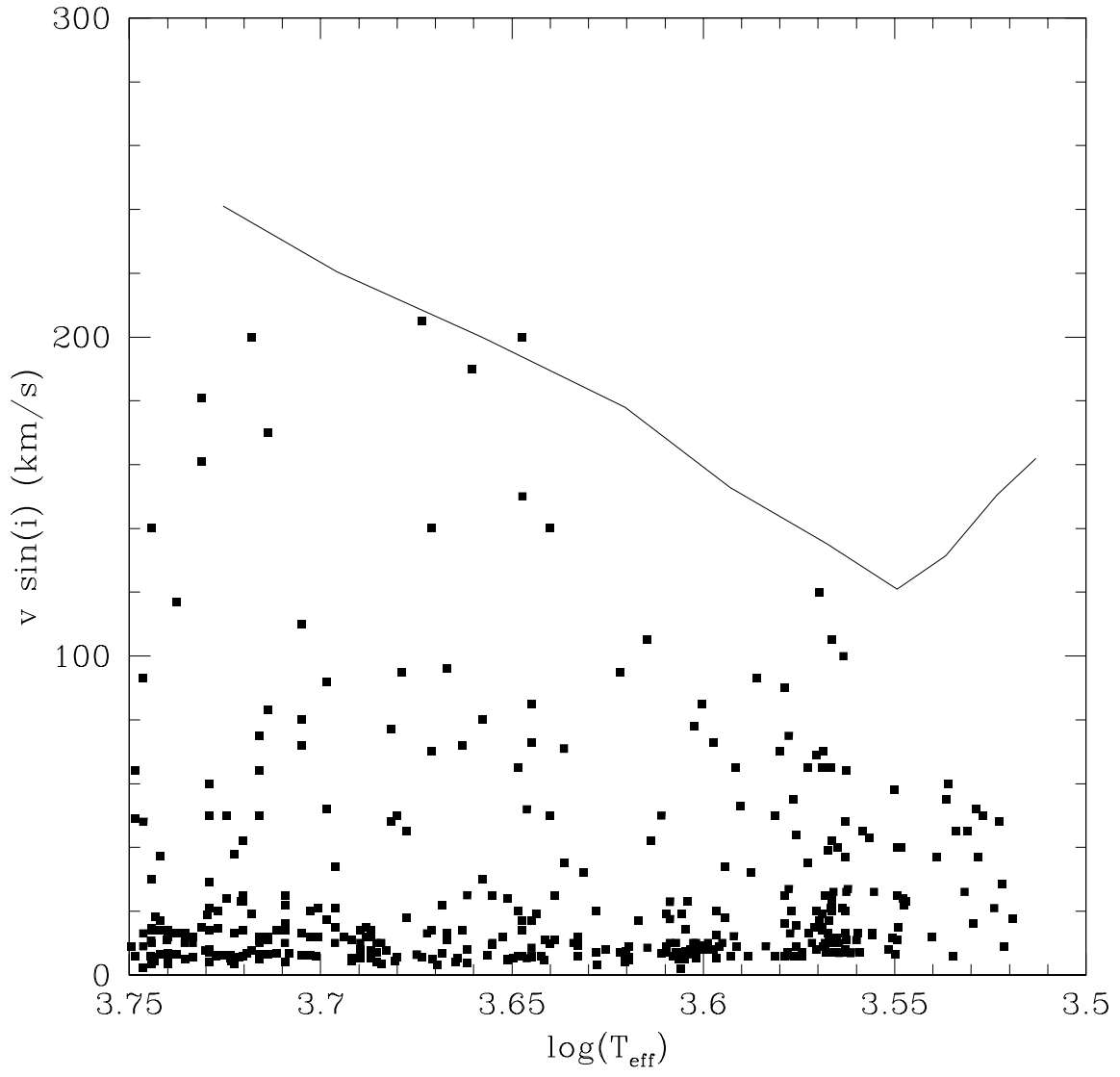
Fig. 2.— Evolutionary tracks for stars with masses between  $0.1 M_{\odot}$  and  $1.0 M_{\odot}$  in steps of  $0.1 M_{\odot}$ . The solid lines are stars without rotation, and the dotted lines are stars which have initial rotation periods of 8 days, and no angular momentum loss.

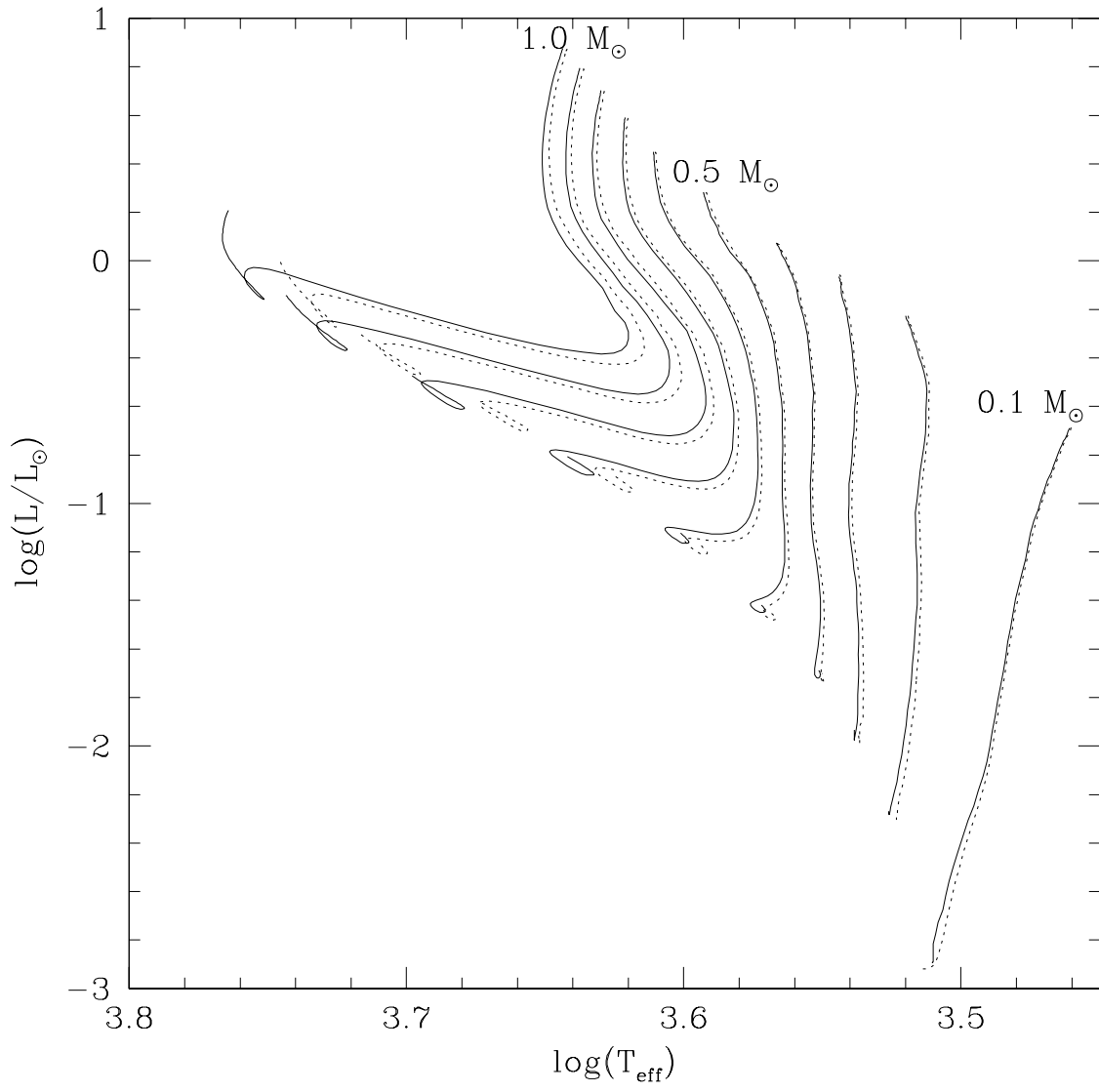
Fig. 3.— Evolutionary tracks for rotating stars under different assumptions about internal angular momentum transport. The solid tracks are stars which have differentially rotating radiative cores and rigidly rotating convection zones, while the dashed lines show the tracks for stars which are constrained to rotate as solid bodies. Stars of the same mass have the same surface rotation rate at the zero age main sequence. Since the low mass stars are fully convective throughout their pre-main sequence lifetime, they always rotate as solid bodies, and so the two tracks are identical. For the higher mass stars, the tracks are the same while the star is on the early pre-main sequence. When the star begins to develop a significant radiative core, however, the two cases have different evolutionary paths.

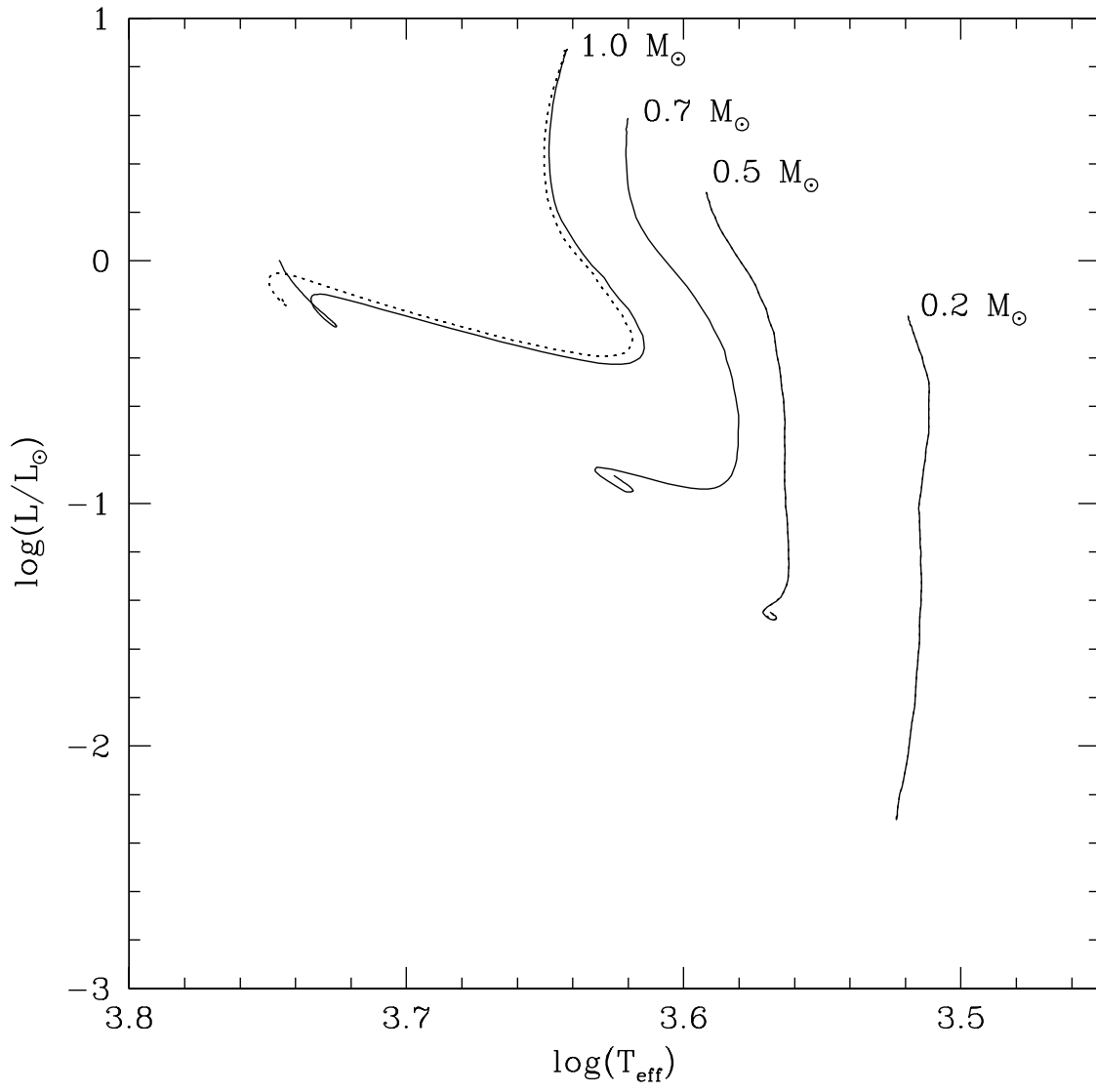
Fig. 4.— The percentage contribution to the total luminosity by the rotational kinetic energy, as a function of age. The maximum contribution is 6%, for the  $1.0 M_{\odot}$  star, but for a short time. For the  $0.1 M_{\odot}$  star, the contribution of rotation kinetic energy lasts the longest time. In either case, the effect on the evolutionary timescale and position in the HR diagram is insignificant.

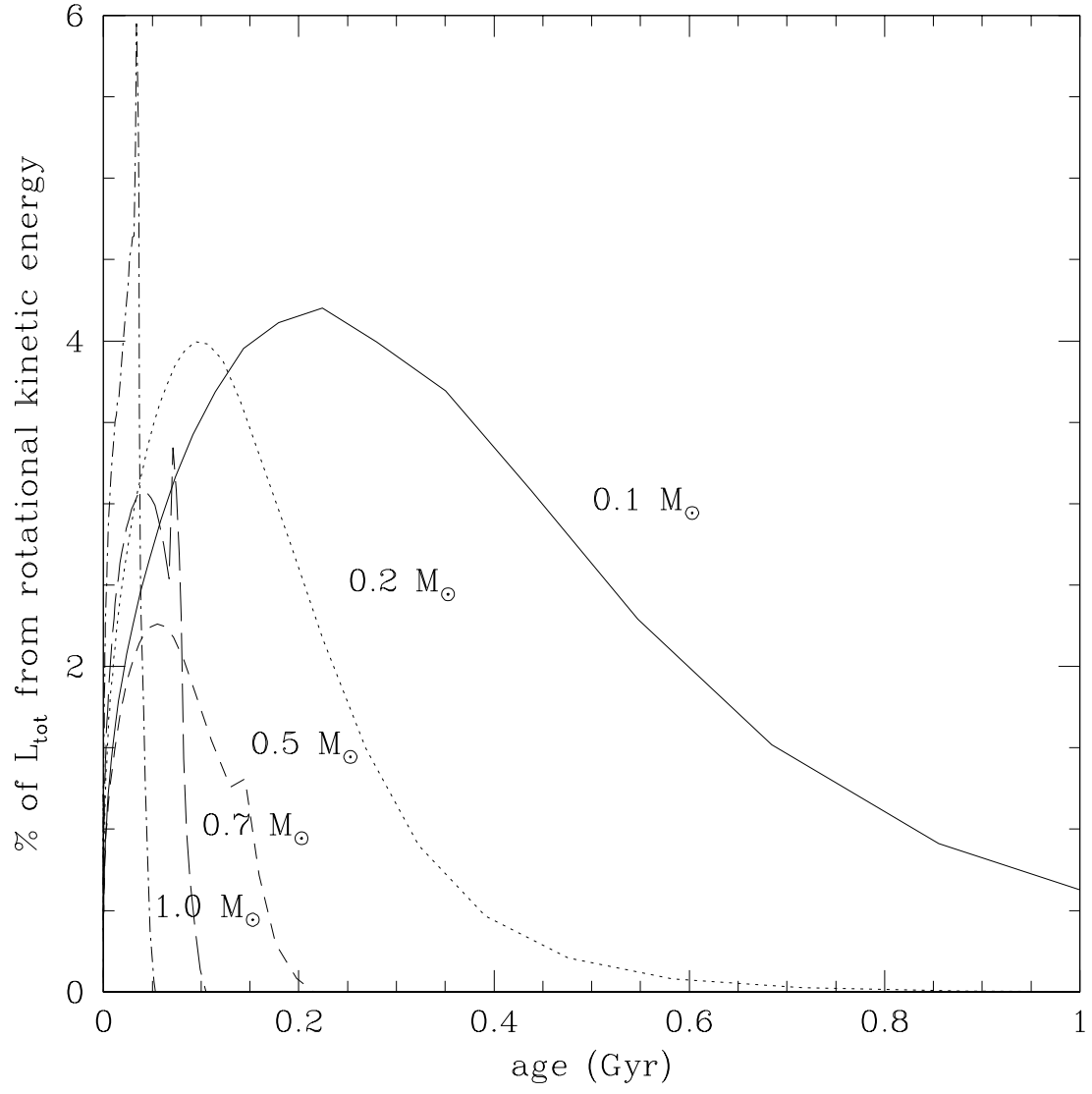
Fig. 5.— Difference between effective temperatures of rotating and non-rotating stars at the same zero age main sequence, as a function of surface rotation velocity. The different lines correspond to stars of different masses, with the highest masses demonstrating the largest difference in temperature. Models which allow for differential rotation are plotted using solid lines, while the solid body rotators are plotted as dashed lines. A difference of a 100 K or more will significantly affect the mapping of stellar mass on observed effective temperature.

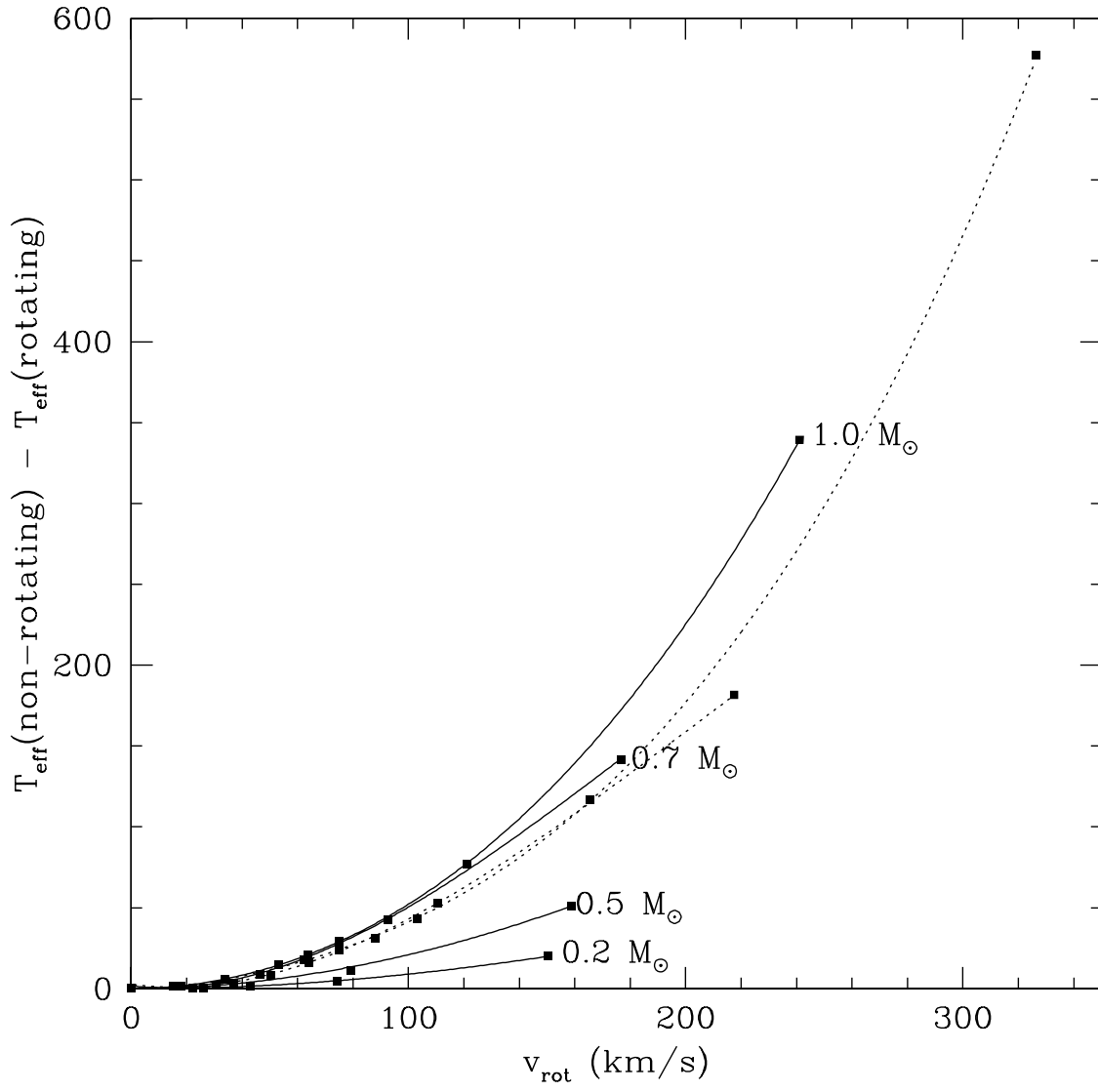
Fig. 6.— Difference between luminosity of rotating and non-rotating stars at the zero age main sequence, as a function of surface rotation velocity. The highest mass stars demonstrate the largest difference in luminosity. However, even for  $1 M_{\odot}$ , the difference in luminosity is not significant, unlike the difference in effective temperature caused by rotation.













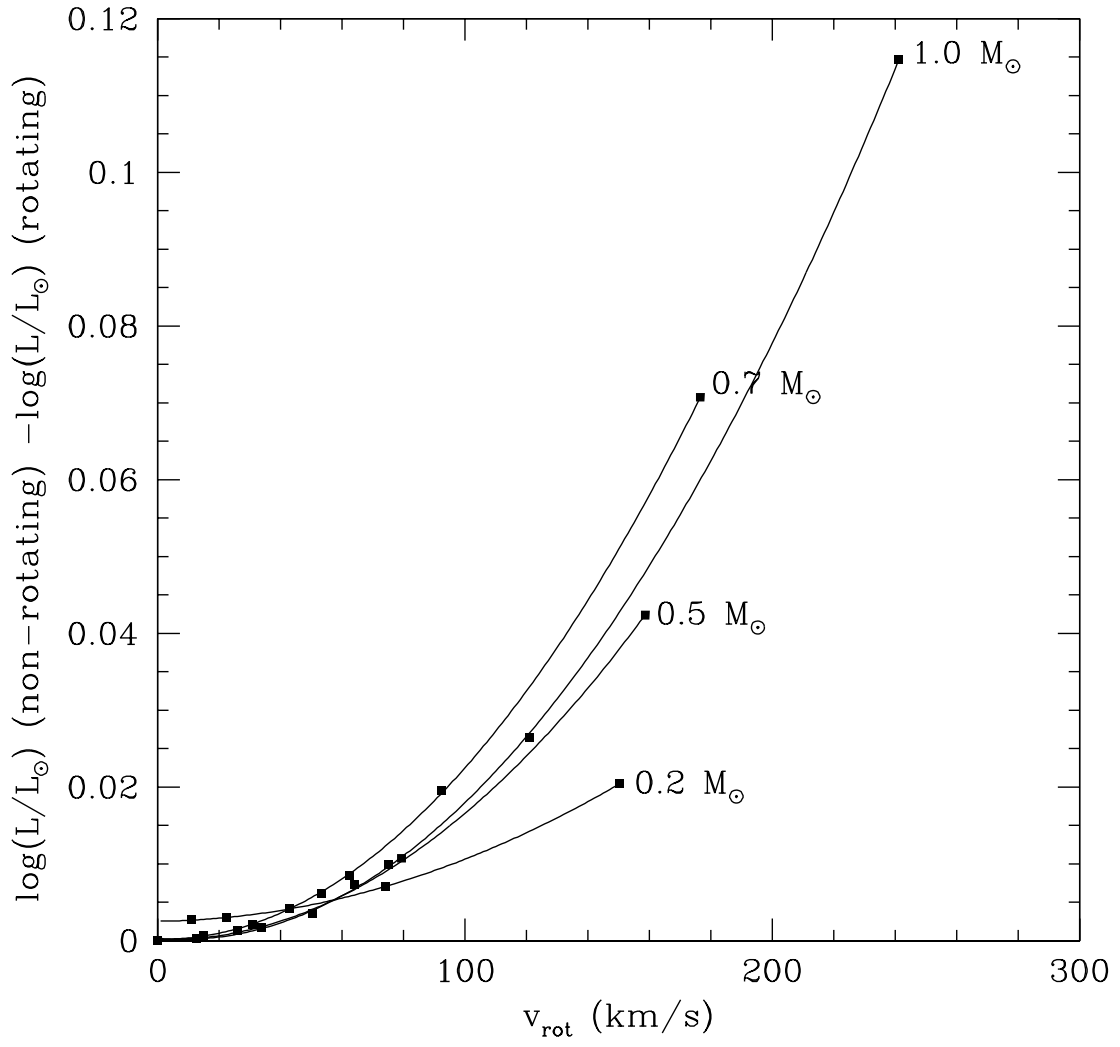


Table 1. Zero Age Main Sequence Information for Rotating Models with an Initial Period of 8 Days, Differential Rotation and no Angular Momentum Loss

Mass ( $M_{\odot}$ )	$\log T_{eff}$	$\log(L/L_{\odot})$	Age (Myr)
0.2	3.526	-2.282	890
0.5	3.572	-1.450	280
0.7	3.634	-0.881	230
1.0	3.752	-0.159	27

Table 2. Polynomial Coefficients:  $T_{eff}^{nrot} - T_{eff}^{rot} = Av_{rot}^3 + Bv_{rot}^2 + Cv_{rot} + D$

Mass ( $M_{\odot}$ )	A	B	C	D
0.2	$-9.43 \times 10^{-7}$	$1.08 \times 10^{-3}$	$-7.71 \times 10^{-3}$	-0.123
0.5	0.0	$1.87 \times 10^{-3}$	$2.98 \times 10^{-2}$	-0.746
0.7	$-1.49 \times 10^{-5}$	$8.13 \times 10^{-3}$	-0.176	1.62
1.0	$5.56 \times 10^{-6}$	$4.37 \times 10^{-3}$	$3.19 \times 10^{-2}$	-0.307
0.7 solid body	$-1.22 \times 10^{-5}$	$7.43 \times 10^{-3}$	-0.217	2.63
1.0 solid body	$1.02 \times 10^{-5}$	$1.53 \times 10^{-3}$	0.184	-2.66